0013-7227/02/$15.00/0
Printed in U.S.A.

The Journal of Clinical Endocrinology & Metabolism 87(1):245–254

A Novel Autocrine Loop Involving IGF-II and the Insulin Receptor Isoform-A Stimulates Growth of Thyroid Cancer

VERONICA VELLA, GIUSEPPE PANDINI*, LAURA SCIACCA, ROSSANA MINEO†, RICCARDO VIGNERI, VINCENZO PEZZINO, AND ANTONINO BELFIORE

Istituto di Medicina Interna e di Malattie Endocrine e del Metabolismo, Cattedra di Endocrinologia, University of Catania, Ospedale Garibaldi (V.V., G.P., L.S., R.M., R.V., V.P.), 95123 Catania, Italy; and Dipartimento di Medicina Sperimentale e Clinica, Cattedra di Endocrinologia, University of Catanzaro, Policlinico Mater Domini (A.B.), 88100 Catanzaro, Italy

The insulin receptor (IR) occurs in two isoforms (IR-A and IR-B) resulting from alternative splicing of exon 11 of the gene. The IR-A isoform is predominantly expressed in fetal tissues and malignant cells and binds IGF-II with high affinity. We previously observed that IRs are overexpressed in thyroid cancer cells; now we evaluated whether these cells preferentially express IR-A and produce IGF-II, which would activate a growth-promoting autocrine loop. The IR content ranged 6.0–52.6 ng/100 μg cell membrane protein in thyroid cancer primary cultures (n = 8) and permanent cell lines (n = 6) *vs.* 1.2–1.7 in normal thyroid cells (n = 11 primary cultures; $P < 0.0001$). IR-A isoform relative abundance ranged from 36–79% in cancer cells (with the highest values in undifferentiated cancers) *vs.* 27–39% in normal cells. Similar results were obtained in normal *vs.* cancer thyroid tissue specimens. IGF-II caused IR autophosphorylation with an ED_{50} of 1.5–40.0 nM in cancer cells *vs.* more than 100 nM in normal cells; IGF-II affinity correlated with the relative abundance of IR-A ($r = 0.628$; $P < 0.0001$). IGF-II was expressed in all cancer cells, highly expressed in anaplastic cells, and less expressed in normal cells.

In conclusion, malignant thyrocytes, especially when poorly differentiated, produce IGF-II and overexpress IR, predominantly as IGF-II-sensitive isoform A. A growth-promoting autocrine loop is activated, therefore, and may affect thyroid cancer biology. (*J Clin Endocrinol Metab* 87: 245–254, 2002)

THYROID CANCER ORIGINATING from the follicular epithelium is represented by well differentiated tumors (papillary or follicular) in over 90% of cases and by undifferentiated tumors in the remaining 10% of cases. Cancer-related mortality ranges from approximately 10% in differentiated tumors up to 100% in undifferentiated tumors (1). The mechanisms determining thyroid cancer aggressiveness and/or dedifferentiation are incompletely understood (2, 3). Pituitary TSH is a major growth factor for differentiated thyroid tumors, but not for those poorly differentiated (2). Even in differentiated tumors, however, TSH suppression may not be sufficient to prevent or inhibit local invasion and metastatic spread, indicating that other factors may be important for tumor progression (1). These factors include numerous growth factors and their tyrosine kinase receptors that may be abnormally overexpressed or constitutively activated in thyroid tumors and influence the tumor biological behavior (4–10).

We recently observed that insulin receptors (IRs) are overexpressed in most thyroid tumors as an early step in thyroid carcinogenesis (11). The role of overexpressed IRs was not clear, because insulin is not locally produced in these tumors. One possibility is that IRs may contribute to transmit the mitogenic signals of insulin homolog IGF-I and IGF-II, produced locally in thyroid cancers (12, 13). IGFs are potent mitogenic and antiapoptotic factors that play a major role in a variety of human malignancies (14). Both IGFs are believed to signal through the IGF-I receptor (IGF-I-R), because they have a low affinity for IR (15, 16). However, we recently identified new mechanisms for the interaction of IGFs with IR. One mechanism involves paracrine IGF-I secretion. IR overexpression may amplify the response of thyroid malignant cells to locally produced IGF-I by increasing the formation of IR/IGF-I-R hybrids (heterodimers formed by one IR α- and β-subunit complex and one IGF-I-R α- and β-subunit complex) (17). Hybrid receptors bind IGF-I with high affinity, similar to that of typical IGF-I-Rs (18). Another mechanism involves direct IR interaction with IGF-II. Although in most cells IGF-II interacts with IR with relatively low affinity, atypical IRs that bind IGF-II with high affinity have been described in human placenta and IM-9 lymphoblasts (19, 20). In addition, in IGF-I-R-deficient mouse fibroblasts that overexpress the IR, IGF-II stimulates cell proliferation via this receptor, which behaves, therefore, as an IGF-II-R (21). The molecular basis of this phenomenon relies on the fact that IGF-II binds with high affinity and activates only one of the two IR isoforms, isoform A (22). The relative abundance of IR isoforms A and B is tightly regulated in a tissue-specific manner by alternative splicing of the 36-bp exon 11 (Ex 11-) of the IR gene (23). Although the IR-B isoform is predominantly expressed in most adult tissues, the IR-A isoform, which binds IGF-II with high affinity, is preferentially expressed in fetal tissues and in certain human malignancies, including breast cancer (22, 24).

Abbreviations: HNMPA, Hydroxy-2-naphthalenylmethyl phosphoric acid triacetoxymethyl ester; IGF-BP, IGF-binding protein; IR, insulin receptor; IGF-I-R, IGF-I receptor; MPR, mannose-6-phosphate receptor; PMSF, phenylmethylsulfonylfluoride.

In the present study we tested the hypothesis that the IR, overexpressed in most thyroid tumors (11, 17), may behave as an IGF-II-R. We investigated, therefore, the expression of IR-A in thyroid cancer cells and its relevance in establishing an autocrine loop with IGF-II. We found that 1) malignant thyrocytes overexpress IR, predominantly as isoform A; 2) autocrine IGF-II production is activated in malignant thyrocytes; 3) IR-A may be directly activated by IGF-II and mediates its mitogenic effect; and 4) both IR-A and IGF-II expression in thyroid cancer correlate with tumor dedifferentiation.

The present data, therefore, identify a novel autocrine loop, involving IGF-II and the IR-A, which may contribute to determine thyroid cancer progression and aggressiveness, especially in undifferentiated carcinomas.

Materials and Methods

Materials

The following materials were purchased: FCS, glutamine, and gentamicin were obtained from Life Technologies, Inc. (Paisley, UK); RPMI 1640 medium, BSA (RIA grade), bacitracin, phenylmethylsulfonylfluoride (PMSF), and porcine insulin were obtained from Sigma (St. Louis, MO); protein A-Sepharose was obtained from Pharmacia Biotech (Uppsala, Sweden); ^{125}I-labeled insulin (SA, 74,000 GBq/mmol) was obtained from Amersham Pharmacia Biotech (Little Chalfont, UK); IGF-I and IGF-II were obtained from Calbiochem (La Jolla, CA); human Del(1–6)IGF-II was obtained from Upstate Biotechnology, Inc. (Lake Placid, NY).

The following antibodies were employed: 1) anti-IR antibodies: MA-20 and MA-51 monoclonal antibodies that recognize IR α-subunit (I. D. Goldfine, San Francisco, CA) (25, 26), CT-1 monoclonal antibody that recognizes the IR β-subunit (27) and 83-7 monoclonal antibody that recognizes the IR α-subunit (K. Siddle, Cambridge UK) (28), and rabbit polyclonal antibody that recognizes the IR β-subunit (Transduction Laboratories, Inc., Lexington, KY); 2) anti-IGF-I-R antibodies: αIR3 monoclonal antibody that recognizes IGF-I-R α-subunit (29) (Oncogene Research, Cambridge, MA), and chicken polyclonal antibody that recognizes IGF-I-R α-subunit (Upstate Biotechnology, Inc.). Antiphosphotyrosine 4G10 and anti-IGF-II (clone S7F2) monoclonal antibodies were purchased from Upstate Biotechnology, Inc. Monoclonal antibody antimannose-6-phosphate receptor (anti-MPR) was purchased from Calbiochem.

Thyroid cell cultures and human tissue specimens

Thyroid primary cell cultures were prepared from both neoplastic (papillary, n = 7; anaplastic, n = 1) and normal thyroid tissue (n = 11) obtained at surgery. Briefly, the tissue was fragmented with a scalpel, suspended in PBS without Ca^{2+} and Mg^{2+}, and digested with a solution of type V collagenase (1 mg/ml) in a 37 C shaking bath for 90 min. The cell suspension, containing intact and fragmented thyroid follicles, was centrifuged (400 $\times$ *g* for 10 min), and the pellet was resuspended in culture medium consisting of RPMI 1640 supplemented with 2 mM glutamine, 5 μg/ml gentamicin, and 3% FCS. Under these conditions follicles formed a monolayer after 1–2 d. The medium was routinely changed every 2 d. To score the degree of nonepithelial cells present in the cultures, epithelial thyroid cells were identified by indirect immunofluorescence staining with anti-Tg and anticytokeratin antibodies as previously described (30). Less than 5% cells were cytokeratin negative, indicating that contamination with nonepithelial cells was low.

Permanent thyroid cancer cell lines (TPC-1, B-CPAP, NPA, FRO, WRO, and ARO) (31–33) and thyroid primary cultures were grown in RPMI 1640 supplemented with 2 mM glutamine, 10% FCS, and 5 μg/ml gentamicin. In all cell lines the medium was routinely changed every 2 d.

Thyroid tissue specimens were collected at surgery, immediately frozen, and stored in liquid nitrogen until processing. Twenty-one thyroid cancer specimens (13 differentiated, 4 less differentiated, and 4 anaplastic) and 5 normal thyroid specimens were used.

Thyroid membrane fraction preparation

The crude thyroid membrane fractions were prepared as follows. Briefly, homogenized tissue specimens or confluent cells were harvested and washed twice with PBS and once with Tris buffer, pH 7.4 (50 mM Tris-HCl, 20 mM benzamidine, 200 μg/ml bacitracin, 30 μg/ml aprotinin, and 10 mM PMSF). They were resuspended in Tris buffer, sonicated three times for 10 sec each time, and centrifuged at 2500 rpm for 10 min at 4 C. Supernatants were removed and saved. The pellets were resuspended in Tris buffer, sonicated three times for 20 sec each time, and centrifuged as in the previous step. Supernatants were removed and added to the previous ones. Combined supernatants were centrifuged at 11,000 rpm for 30 min at 4 C. The pellets were resuspended in Tris buffer using a syringe with a 25-gauge needle. The suspensions were aliquoted in microfuge tubes and centrifuged for 30 min. Supernatants were removed, and pellets were stored at −80 C.

Cell monolayers, tissues, and membrane fractions were solubilized with 50 mM HEPES buffer, pH 7.6, containing 1 mM PMSF, 1 mg/ml bacitracin,150 mM NaCl, 2 mM sodium orthovanadate, and 1% Triton X-100 for 60 min at 4 C. The solubilized material was then centrifuged at 10,000 $\times$ *g*, and the supernatant was frozen at −80 C until assayed. The protein content in the cellular extracts was measured by the bicinchoninic acid method (Pierce Chemical Co., Rockford, IL).

IR and isoform measurements

IR ELISA. IRs were captured by incubating membrane fraction lysates from cells or tissues in Maxisorp immunoplates (Nunc, Roskilde, Denmark) precoated with 2 μg/ml MA-20, as previously described (24). After washing, the immunocaptured receptors were incubated with the biotinylated anti-IR CT-1 antibody (0.3 μg/ml in 50 mM HEPES-buffered saline, pH 7.6, containing 0.05% Tween 20, 1% BSA, 2 mM sodium orthovanadate, 1 mg/ml bacitracin, and 1 mM PMSF) and then with peroxidase-conjugated streptavidin. The peroxidase activity was determined colorimetrically by adding 100 μl 3,3′,5,5′-tetramethylbenzidine (0.4 mg/ml in 0.1 M citrate-phosphate buffer, pH 5.0, with 0.4 μl/ml 30% H_2O_2). The reaction was stopped by the addition of 1 M H_3PO_4, and the absorbance was measured at 450 nm.

IR isoform relative abundance was measured by RT-PCR, as previously described (24, 34). Briefly, total cellular RNA was isolated from each cell line or specimen using TRIzol RNA isolation reagent (Life Technologies, Inc., Gaithersburg, MD). First strand cDNA synthesis was performed on 4–8 μg total RNA using Moloney murine leukemia virus reverse transcriptase (Life Technologies, Inc.) and random hexamer primers (Pharmacia Biotech) in a total volume of 40 μl 75 mM KCl, 50 mM Tris-HCl (pH 8.3), 3 mM $MgCl_2$, and 0.5 mM dNTPs.

cDNA synthesis reaction (5-μl volume) was combined in a 50-μl final reaction volume for PCR amplification containing 0.2 μM oligonucleotide primers spanning nucleotides 2229–2250 (5′-AAC-CAG-AGT-GAG-TAT-GAG-GAT-3′) and 2844–2865 (5′-CCG-TTC-CAG-AGC-GAA-GTG-CTT-3′) of the human IR and 1.25 U *Taq* DNA polymerase (AmpliTaq, Perkin-Elmer Corp.). PCR amplification was carried out for 30 cycles of 15 sec at 95 C, 30 sec at 60 C, and 45 sec at 72 C, using a DNA thermal cycler (Perkin-Elmer Corp.). Products of PCR amplification were resolved by electrophoresis on 5% polyacrylamide gels. The electrophoretic analysis showed the 600- and 636-bp DNA fragments representing $Ex11^-$ and $Ex11^+$ IR isoforms, respectively. Gels were silver stained, and band density was quantified by scanning densitometry.

Ligand-binding assay for IR

Membrane fractions were solubilized as described above, and IR was immunocaptured by incubating for 22 h in Maxisorp immunoplates Break-Apart (Nunc, Roskilde, Denmark), precoated with 2 μg/ml anti-IR 83-7. After washing, the immunocaptured receptors were incubated with [^{125}I]insulin (10 pM in 50 mM HEPES-buffered saline, pH 7.6, containing 0.05% Tween 20, 1% BSA, 2 mM sodium orthovanadate, 1 mg/ml bacitracin, and 1 mM PMSF) in the presence or absence of increasing concentrations of various unlabeled ligands (insulin, IGF-I, or IGF-II). After 2 h at room temperature, plates were washed, and the radioactivity in each well was counted in a γ-counter.

IR autophosphorylation: ELISA

IR autophosphorylation in intact cells. Ligand-activated IR autophosphorylation in intact cells was measured as previously described (35). Cells in monolayer cultures were stimulated with increasing doses (0–100 nM) of insulin, IGF-II, or IGF-I for 5 min at 37 C. Cells were then solubilized, and receptors were captured by incubating cell lysates (containing ~2 ng receptor) in Maxisorp plates precoated with antireceptor antibody MA-20. After washing, a biotinylated antiphosphotyrosine antibody (4G10 αPY from Upstate Biotechnology, Inc., Lake Placid, NY; 0.3 μg/ml in 50 mM HEPES-buffered saline, pH 7.6, containing 0.05% Tween 20, 1% BSA, 2 mM sodium orthovanadate, 1 mg/ml bacitracin, and 1 mM PMSF) was added to reveal phosphorylated receptors by the peroxidase-conjugated streptavidin method. Peroxidase activity was determined colorimetrically by adding 100 μl 3,3′,5,5′-tetramethylbenzidine (0.4 mg/ml in 0.1 M citrate-phosphate buffer, pH 5.0, with 0.4 μl/ml of 30% H_2O_2). The reaction was stopped by the addition of 1 M H_3PO_4, and the absorbance was measured at 450 nm.

IR phosphorylation in isolated receptors. IR kinase activity was also measured in purified receptors. Membrane fractions were solubilized as described above and IR immunocaptured in Maxisorp plates coated with the anti-IR antibody MA-20. The immunopurified receptors were then stimulated with various concentrations of either insulin or IGFs in the presence of ATP (10 μM), $MgCl_2$ (10 mM), and $MnCl_2$ (2 mM). After washing, the phosphorylated proteins were incubated with an antiphosphotyrosine-biotin-conjugated antibody, and the reaction was detected as described above.

IR autophosphorylation: Western blot analysis

Confluent cells were incubated in serum-free medium for 48 h, stimulated with 10 nM insulin, IGF-II, or IGF-I for 5 min at 37 C, and solubilized in RIPA buffer [50 mM Tris (pH 7.4), 1% NP-40, 0.25% sodium deoxycolate, 150 mM NaCl, 1 mM EGTA (pH 8.0), 1 mM PMSF, 10 μg/ml aprotinin, 10 μg/ml leupeptin, 10 μg/ml pepstatin, 2 mM Na orthovanadate, and 1 mM NaF]. Cell lysates were immunoprecipitated with either anti-IR (MA-20 monoclonal), or anti-IGF-I-R (α-IR3 monoclonal) antibodies. Immunoblottings were performed using 4G10 antiphosphotyrosine antibody. To show the amounts of receptors loaded in each lane, filters were first subjected to stripping in Tris-HCl buffer (62.5 mM, pH 6.7) containing 2% SDS and 100 mM β-mercaptoethanol for 30 min at 50 C. Next, the half-filter containing IRs was reprobed with an anti-IR β-subunit polyclonal antibody, and the half-filter containing IGF-I-Rs was reprobed with an anti-IGF-I-R α-subunit polyclonal antibody. All immunoblots were revealed by an ECL method (Amersham Pharmacia Biotech), autoradiographed, and subjected to densitometric analysis.

Measurement of IGF-I/II production

IGF-I and IGF-II mRNA content in human thyroid cancer cell lines and tissue specimens was evaluated by PCR. Total RNA was prepared from cells and tissue specimens using TRIzol RNA isolation reagent (Life Technologies, Inc.). First strand cDNA synthesis was performed on 4–8 μg total RNA using Moloney murine leukemia virus reverse transcriptase (Life Technologies, Inc.) and random hexamer primers (Amersham Pharmacia Biotech) in a total volume of 40 μl 75 mM KCl, 50 mM Tris-HCl (pH 8.3), 3 mM $MgCl_2$, and 0.5 mM dNTPs. PCR amplification was performed with 5 μl cDNA, adding 1.25 U *Taq* polymerase (Perkin-Elmer Corp.), 2.5 mM specific primers, 2.5 mM $MgCl_2$, and 0.2 mM dNTPs. The following primer sequences were used: 5′-3′, GAA-GTC-GAT-GCT-GGT-GCT-TC; and 3′-5′, CTT-CCG-ATT-GCT-GGC-CAT-CT. Conditions for PCR were: 94 C for 30 sec, 60 C for 30 sec, and 72 C for 30 sec for 30 cycles. PCR products were resolved by electrophoresis on 5% polyacrylamide gels and silver stained.

IGF-II protein secreted by cultured thyroid cancer cells in the conditioned medium was measured by a commercial immunoradiometric assay that detects only the IGF-II mature form (BIOS, Naples, Italy) and was expressed as nanograms of IGF-II secreted per h/10^6 cells.

Cell growth studies

To evaluate to what extent the mitogenic effect of IGF-II on thyroid cancer cells occurred via the IR, the growth of B-CPAP and ARO cells was measured in the presence or absence of the anti-IR blocking antibody MA-51 as previously described (36). Briefly, cells (1.5×10^3) were seeded in 96-well plates. After 24 h the medium was removed and replaced with medium containing 1% charcoal-stripped FCS. After an additional 24 h various concentrations of insulin, IGF-II, or IGF-I (0–10 nM) were added in fresh medium in the presence of a 5-fold molar excess of MA-51, aIR-3, or both antibodies. Normal mouse IgGs were used in control wells. Cell growth was measured after 4 d by measuring the rate of tetrazolium salts reduction to formazan (3-[4,5-dimethylthiazol-2-yl]-2,5-diphenyltetrazolium bromide, Amersham Pharmacia Biotech), which is proportional to the number of living cells (37). At the end of the incubation the absorbance was read at 540 nm.

To investigate the autocrine effect of IGF-II two different methods were used: 1) B-CPAP or ARO cells were cultured in serum-free medium, and their growth rate was measured in the presence of a blocking anti-IGF-II monoclonal antibody at 2 μg/ml concentration or in the presence of an unrelated monoclonal antibody (control cultures); 2) in serum-starved cells growth was also evaluated at 2, 4, and 6 d in the presence or absence of 10 nM exogenous IGF-II with or without the addition to the culture medium of 1 μg/ml hydroxy-2-naphthalenylmethyl phosphoric acid triacetoxymethyl ester (HNMPA), a specific IR tyrosine kinase inhibitor (38).

MPR Western blot analysis

To measure IGF type II receptor (MPR), membrane proteins extracted from thyroid cells were separated by SDS-PAGE (7.5% polyacrylamide) under nonreducing conditions. Immunoblotting was performed using an anti-MPR antibody. The immunoblot was revealed by an ECL method (Amersham Pharmacia Biotech), autoradiographed, and subjected to densitometric analysis.

Statistical analysis

Differences between means were evaluated using paired *t* test, Mann-Whitney test, or one-way ANOVA, as indicated in *Results*. The ability of IGF-II to activate the IR and the relative abundance of IR-A were correlated by linear regression analysis. The statistical program PRISM (GraphPad Software, Inc., San Diego, CA) was used.

Results

IR overexpression and predominance of IR isoform A in malignant thyrocytes: relationship with the degree of cancer differentiation

IRs were measured by ELISA in cell membrane preparations from both thyroid cell primary cultures and a variety of thyroid malignant cells in permanent culture. Primary cultures were obtained from either normal thyroid (n = 11) or thyroid carcinomas (papillary, n = 7; anaplastic, n = 1). The median IR content was 8.7- to 37.6-fold higher in malignant thyrocytes compared with normal thyrocytes, which expressed the IR at 1.2–1.7 ng/100 μg cell membrane protein (Table 1).

The relative abundance of the two IR isoforms was then evaluated by RT-PCR in both normal and cancer thyroid cells in primary cultures. Interestingly, isoform A (IR-A) was often predominant in cancer cells, whereas isoform B (IR-B) was predominant in normal cells. The proportion of IR-A increased from 27–39% in normal thyrocytes to 36–65.2% in papillary cancer cells and 69.8% in anaplastic cancer cells (Table 1 and Fig. 1).

Six permanent thyroid cancer cell lines (papillary, n = 3; follicular, n = 2; anaplastic, n = 1) were also evaluated. Similarly to what observed in primary cultures, in these cancer cells both the IR content and the IR-A relative abundance were clearly increased compared with those in normal

TABLE 1. IR content and relative abundance of isoform A (IR-A) in primary cultures obtained from normal thyroid and thyroid carcinomas

Thyroid cells	IR (ELISA; ng/100 μg protein)	IR-A (RT-PCR; %)
Normal thyroid cells (n = 11)		
Mean ± SD	1.5 ± 0.2	32.6 ± 3.8
Range	1.2–1.7	27–39
Median	1.4	31.6
Papillary cancer cells (n = 7)		
Mean ± SD	13.5 ± 7.1	52.3 ± 11.6
Range	4.3–22.8	36–65.2
Median	12.2	57.2
Anaplastic cancer cells (n = 1)	52.6	69.8 ± 8.4

IR content: normal *vs.* cancer (papillary + anaplastic), $P = 0.0002$; normal *vs.* papillary cancer, $P = 0.0003$. IR-A relative abundance: normal *vs.* cancer (papillary + anaplastic), $P = 0.0003$; normal *vs.* papillary cancer, $P = 0.0006$ (by Mann-Whitney test).

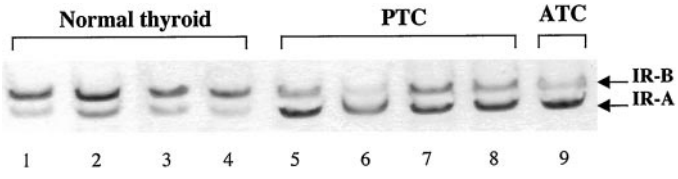

FIG. 1. IR isoform mRNA expression (RT-PCR) in normal and cancer thyroid cells. Primary thyroid cell cultures (lanes 1–4) predominantly expressed the IR-B isoform, whereas primary cultures of thyroid cancer cells (lanes 5–9) predominantly expressed the IR-A isoform. The predominance of IR-A was more marked in anaplastic thyroid cancer cells (ATC; lane 9) than in papillary thyroid cancer cells (PTC; lanes 5–8).

TABLE 2. IR content and relative abundance of isoform A (IR-A) in normal thyroid cells and in established thyroid cancer cell lines

Thyroid cells	IR (ELISA; ng/100 μg protein)	IR-A (RT-PCR; %)
Normal thyroid cells (n = 11)	1.5 ± 0.2	32.6 ± 3.8
Papillary cancer cells		
TPC-1	6.0 ± 0.6	37.7 ± 0.6
NPA	12.0 ± 1.2	43.1 ± 4.4
B-CPAP	33.2 ± 11.2	69.8 ± 4.3
Median	12	43.1
Follicular cancer cells		
FRO	6.6 ± 2.1	36.2 ± 1.1
WRO	19.6 ± 3.1	45.1 ± 1.9
Median	12.2	40.7
Anaplastic cancer cells		
ARO	10.2 ± 1.2	79.3 ± 5.6

IR content: normal *vs.* cancer (total), $P = 0.0011$. IR-A relative abundance: normal *vs.* cancer (total), $P = 0.0042$ (by Mann-Whitney test).

thyrocytes (Table 2). In particular, the IR content reached levels up to 23 times higher than normal (in B-CPAP cells), and IR-A relative abundance increased up to 80% (in the anaplastic cells ARO; Table 2).

Autocrine IGF-I/II production and high affinity IR activation by IGF-II in malignant thyrocytes

IGF-I/II secretion in cultured thyrocytes. We have previously shown that IR-A, but not IR-B, binds IGF-II with high affinity (22). As thyroid cancer cells overexpress IR-A, we next evaluated whether these cells produce IGF-II, thus raising the possibility of an autocrine loop by which IGF-II stimulates cell growth via the overexpressed IR-A.

We first evaluated IGF-I and IGF-II mRNA in both primary cultures and permanent cell lines by RT-PCR. IGF-I mRNA was absent in all thyroid cells, both normal and malignant, although it was present in control osteosarcoma cells (data not shown). At variance with IGF-I, IGF-II mRNA was found in all cancer cell lines and in 7 of 11 primary cultures from normal thyroid (data not shown). IGF-II protein secretion was also measured in cell-conditioned medium by an immunoradiometric assay. Median values of IGF-II protein secretion were approximately 5- to 7-fold higher in differentiated thyroid cancer cells (from either papillary or follicular cancer) than in normal thyroid cells. Again, as for the relative abundance of IR-A, IGF-II secretion was most elevated in undifferentiated cancer cells (Table 3).

IGF-II binding and activation of IR in malignant thyrocytes: relationship with the relative abundance of IR-A. As malignant thyrocytes produce IGF-II and overexpress the IR-A, we then evaluated the ability of IGF-II to bind and activate IRs immunopurified from these cells. For this purpose we studied three cancer cell lines (CA 18-3, B-CPAP, and ARO) with increasing IR-A relative abundance (approximately 50%, 70%, and 80%, respectively) and compared them with normal thyrocytes (IR-A, ~30%). To avoid the possible interference of IGF-binding proteins (IGF-BPs), cell membrane fractions were extracted and solubilized, and IRs were immunocaptured onto Maxisorp plates. ^{125}I-Labeled insulin binding was displaced with insulin, IGF-I, or IGF-II. Competition for labeled insulin binding revealed a low affinity of IGF-II for the IR obtained from normal thyrocytes and containing only approximately 30% IR-A. In contrast, labeled insulin binding was displaced by IGF-II with a high affinity in IRs extracted from B-CPAP and ARO cells (containing the IR-A isoform up to 70–80%; Fig. 2).

The ability of IGF-II to activate IR autophosphorylation was then studied in normal thyrocytes, CA 18-3, B-CPAP, and ARO cells both *in vitro* in immunocaptured receptors and in intact cells. IRs were immunocaptured using MA-20 antibody, and receptor autophosphorylation was measured by ELISA after stimulation with insulin, IGF-I, or IGF-II in the presence of ATP and cofactors. IGF-II activated IR with high affinity in cells that express predominantly IR-A (ED_{50} = 2.7 and 2.0 nM IGF-II in B-CPAP and ARO, respectively), whereas it activated IR with low affinity in normal thyrocytes. Intermediate values (ED_{50} = 16.0 nM IGF-II) were observed in CA 18-3 cells. Very similar data were obtained when intact cell monolayers were incubated with the different ligands, and IR autophosphorylation was detected by ELISA (data not shown). Western blot analysis carried out in normal thyrocytes, CA 18-3, and ARO cells also showed that the ability of IGF-II to activate the IR was related to the IR-A relative abundance, being minimal in primary cultures of normal thyroid cells, very high in undifferentiated cancer cells (ARO), and intermediate in differentiated thyroid cancer cells (CA 18-3; Fig. 3).

Half-maximal dose (ED_{50}) IR activation by IGF-II was then studied in the 14 cancer cell lines and 11 preparations of normal thyrocytes previously studied for IR isoform expres-

TABLE 3. Relative abundance of IR-A, IR autophosphorylation in response to either insulin or IGF-II (ED_{50}), and IGF-II production in cultured normal and malignant thyrocytes

Thyroid cells	% IR-A (RT-PCR)	IR autophosphorylation (ED_{50})		IGF-II production in conditioned medium (ng/10^6 cells·h)
		Insulin (nM)	IGF-II (nM)	
Normal thyroid cells (primary cultures, n = 11)				
Mean ± SD	32.6 ± 3.8	1.4 ± 0.31	>100	3.1 ± 2.8[a]
Range	27–39	1.1–1.8		1.1–8.9[a]
Median	31.6	1.25		2.1[a]
Papillary cancer cells (primary cultures, n = 10; n = 7; cell lines, n = 3)				
Mean ± SD	55.3 ± 11.16	1.1 ± 0.21	10.4 ± 12.64	12.5 ± 8.1
Range	36.0–69.8	0.9–1.2	2.8–40	4.3–27.7
Median	58.8	1.05	4.8	10.7
Follicular cancer cells (cell lines, n = 2)				
Mean ± SD	40.7 ± 6.3	1.0 ± 0.26	13.7 ± 2.1	14.7 ± 0.6
Range	36.2–45.1	0.7–1.2	12.4–15.0	14.3–15.1
Median	40.65	0.9	13.7	14.7
Anaplastic cancer cells (n = 2; primary cultures, n = 1; cell lines, n = 1)				
Mean ± SD	74.6 ± 6.72	0.7 ± 0.04	1.6 ± 0.07	40.0 ± 21.9
Range	69.8–79.3	0.7–0.75	1.5–1.6	24.5–55.5
Median	74.6	0.725	1.6	40.0

IR-A relative abundance: normal *vs.* cancer (total), $P < 0.0001$; papillary + follicular *vs.* anaplastic cancer, $P = 0.0383$ (by Mann-Whitney test). IGF-II production: normal *vs.* cancer (total), $P = 0.004$; normal *vs.* papillary + follicular cancer, $P = 0.009$; papillary + follicular *vs.* anaplastic cancer, $P = 0.060$ (by Mann-Whitney test).

[a] Values in the 7 of 11 IGF-II-positive cultures.

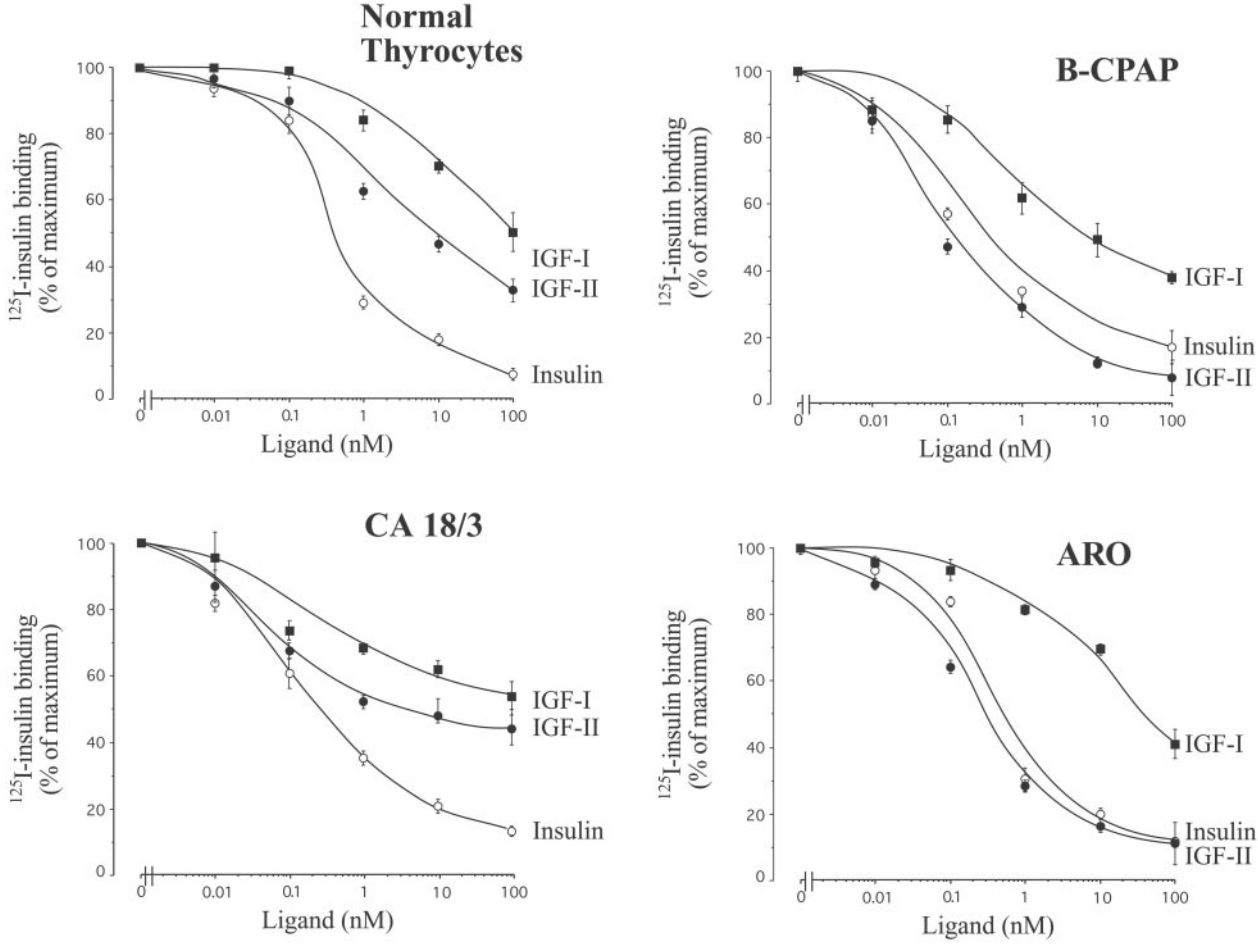

FIG. 2. IGF-II binding to immunopurified IR. IRs from lysates of either normal thyrocytes or CA 18-3, B-CPAP, and ARO malignant cells were immunocaptured, and ^{125}I-labeled insulin binding was displaced with insulin or IGF-I or IGF-II. Cell lines with a predominance of IR-A revealed high affinity binding for IGF-II compared with normal thyrocytes that have a low IR-A relative abundance.

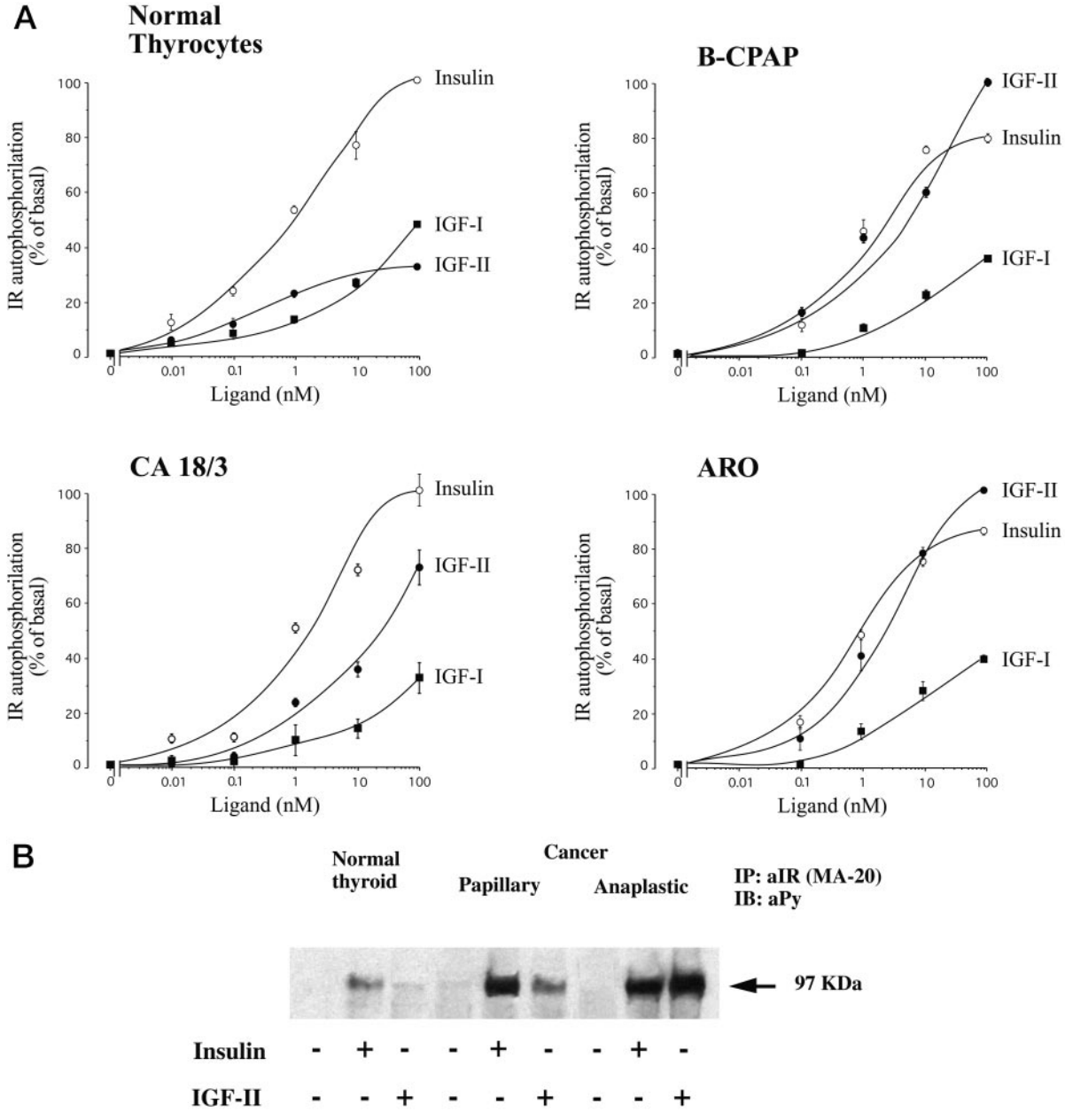

FIG. 3. IGF-II-induced IR autophosphorylation in receptors immunopurified by thyroid cells with different IR-A relative abundance. A, *In vitro* autophosphorylation of immunopurified IR. IRs immunocaptured with antibody MA-20 from lysates of unstimulated cells were stimulated *in vitro* with various concentrations of either insulin or IGFs in the presence of ATP and cofactors. IR activation was measured as described in *Materials and Methods*. B, Western blot analysis. Primary cultures of normal thyroid cells, papillary cancer cells, and anaplastic cancer cells, incubated in serum-free medium for 16 h, were stimulated with either insulin or IGF-II (10 nM) and lysed in 1 ml lysis buffer. Samples were then immunoprecipitated with the anti-IR monoclonal antibody MA-20 and subjected to Western blot analysis using an anti-PY antibody to detect receptor autophosphorylation. In both A and B IGF-II-induced IR autophosphorylation was directly related to the relative abundance of the IR-A isoform, being minimal in normal thyroid cells (IR-A, 27.0%), high in anaplastic cancer cells (IR-A, 79.1%), and intermediate in differentiated cancer cells (IR-A, 48.4%).

sion. Cells cultured in monolayers were exposed to increasing doses of insulin, IGF-I, or IGF-II, and IR autophosphorylation was detected by ELISA. IR autophosphorylation in response to insulin occurred with a similar ED_{50} in normal and malignant thyrocytes (1.1–1.8 *vs.* 0.7–1.2 nM, respectively; Table 3). In contrast, IR autophosphorylation in response to IGF-II differed in malignant *vs.* normal thyrocytes. In normal thyrocytes IGF-II induced IR autophosphorylation with an affinity that was always less than 1% that of insulin (ED_{50} = >100 nM), whereas in all thyroid cancer cells IGF-II activated IR autophosphorylation with an ED_{50} much closer to that of insulin. Median ED_{50} values were 4.8 nM in papillary cancer cells, 13.7 nM IGF-II in follicular cancer cells, and 1.6 nM in anaplastic cancer cells (Table 3).

In the 25 cell cultures studied (Table 3), the relative affinity of IGF-II for the IR (calculated as the percentage of insulin

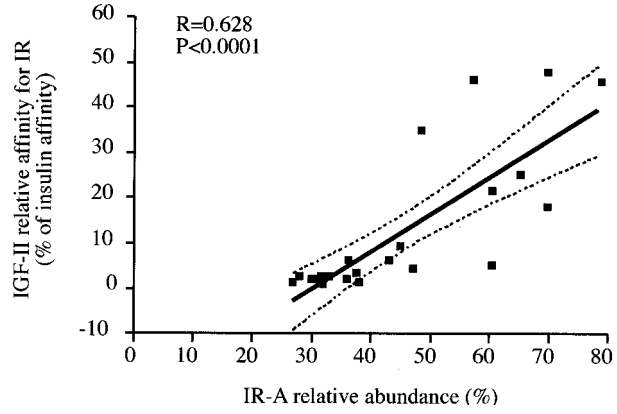

FIG. 4. Correlation between IR autophosphorylation by IGF-II and IR-A relative abundance. In 25 thyroid cell cultures (normal, n = 11; cancer, n = 14) a correlation (linear regression analysis) was observed between the IGF-II relative affinity for the IR (calculated as the percentage of insulin ED_{50}/IGF-II ED_{50} for stimulation of IR autophosphorylation) and the relative abundance of the IR-A isoform as determined by RT-PCR.

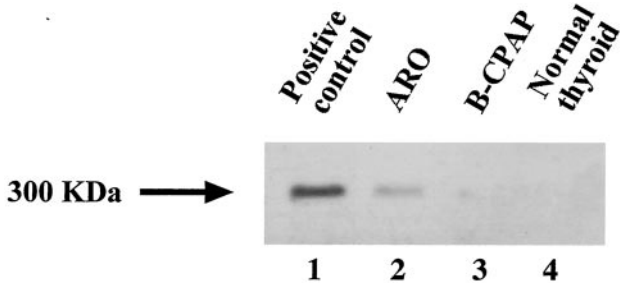

FIG. 5. IGF-II/MPR content in thyroid cell lines. Western blot analysis of MPR in primary culture of normal thyroid cells (2), papillary cancer cells B-CPAP (3), and anaplastic cancer cells ARO (4). As a positive control, HepG2 cells were used (1). Membrane fractions were solubilized and subjected to Western blot analysis using an anti-MPR antibody to detect receptor content.

ED_{50}/IGF-II ED_{50} for stimulation of IR autophosphorylation) was correlated with the relative abundance of IR-A expression ($r = 0.628$; $P = 0.0001$; Fig. 4). IGF-I was always less than 1% as effective as insulin in stimulating IR autophosphorylation (data not shown).

Cell growth studies

IGF-II stimulation of thyroid cancer cell growth: role of the IR-A. To evaluate whether IR-A overexpression may have a role in mediating a mitogenic response to IGF-II in thyroid cancer cells, we studied B-CPAP (papillary cancer) and ARO cells (undifferentiated cancer), which predominantly express IR-A (approximately 70% and 80%, respectively). The biological effects of IGF-II in target cells may be regulated by mechanisms that influence IGF-II bioavailability, including the expression of IGF-II/MPR, which decreases IGF-II bioavailability, and the presence of IGF-BPs, which may either increase or decrease IGF-II bioavailability. Therefore, we first studied the expression of IGF-II/MPR in these cell lines. Western blot analysis showed that IGF-II/MPR was undetectable in normal thyroid cells and expressed at low levels in B-CPAP and ARO cell lines (Fig. 5). To evaluate the possible effect of IGF-BPs, serum-starved cells were exposed for 4 d to different doses of IGF-II or del(1–6)IGF-II, a truncated IGF-II analog that does not bind to IGF-BPs. In B-CPAP and ARO cell lines both ligands stimulated 3-[4,5-dimethylthiazol-2-yl]-2,5-diphenyltetrazolium bromide incorporation in a dose-dependent manner. The maximal growth effect was observed at 10 nM for each ligand and ranged from 152–169% in B-CPAP cells and from 174–207% in ARO cells, with no difference between the two ligands. The very similar growth response obtained with both IGF-II and del(1–6)IGF-II suggests that IGF-BPs do not have a major role in regulating the IGF-II growth response in this system.

TABLE 4. Effect of receptor blockade on insulin-, IGF-I-, or IGF-II-induced cell growth in B-CPAP cells

Conditions	OD (540 nm)	% of basal	P^a
Basal	0.51 ± 0.19	100	
Insulin	0.98 ± 0.04	191.9	
Insulin + control Ab	0.95 ± 0.07	185.9	
Insulin + MA-51	0.75 ± 0.02	147.3	0.001
Insulin + αIR3	0.94 ± 0.06	184.1	0.204
Insulin + MA-51 + αIR3	0.74 ± 0.04	144.6	0.007
Basal	0.51 ± 0.19	100	
IGF-II	0.98 ± 0.02	190.9	
IGF-II + control Ab	0.95 ± 0.05	185.4	
IGF-II + MA-51	0.78 ± 0.05	152.8	0.005
IGF-II + αIR3	0.83 ± 0.02	162.5	0.008
IGF-II + MA-51 + αIR3	0.67 ± 0.03	132.0	<0.001
Basal	0.51 ± 0.19	100	
IGF-I	1.03 ± 0.04	201.9	
IGF-I + control Ab	0.99 ± 0.06	194.1	
IGF-I + MA-51	1.01 ± 0.05	198.0	
IGF-I + αIR3	0.71 ± 0.02	139.2	<0.001

Results are the mean ± SEM of three separate experiments.
[a] Statistical significance is calculated *vs.* growth stimulation in the presence of control IgG (by paired *t* test).

To evaluate the relative contribution of either IR-A or IGF-I-R to IGF-II-induced growth, cells were incubated with 10 nM insulin, IGF-II, or IGF-I. Cell growth in response to each ligand was measured in the presence of MA-51 (IR-blocking antibody), αIR3 (IGF-I-R-blocking antibody), or a combination of these two antibodies. An unrelated monoclonal antibody was used as control.

In B-CPAP cells, insulin-induced cell growth was effectively blocked by MA-51 ($P < 0.001$), but not by αIR-3 (Table 4). A combination of the two antibodies was as effective as MA-51 alone. In contrast, IGF-II-induced growth was significantly inhibited by either MA-51 or αIR-3 to a similar extent ($P = 0.025$), suggesting that both IR-A and IGF-I-R are similarly important in mediating IGF-II effects in B-CPAP cells (Table 4). The two antibodies together were more effective than either antibody alone and almost completely blocked the growth response to IGF-II. As expected, IGF-I-induced growth was significantly decreased by αIR-3 ($P < 0.001$), but not by MA-51. A combination of the two antibodies was as effective as αIR-3 alone (Table 4). Similar results were obtained in ARO cells (data not shown).

Blockade of the autocrine IGF-II/IR-A loop: effect on cell growth. As both B-CPAP and ARO cells produce substantial amounts of IGF-II (27.7 ± 0.4 and 24.5 ± 2.6 ng/10^6 cells·h, respectively), but not IGF-I, we evaluated the effect of blockade of

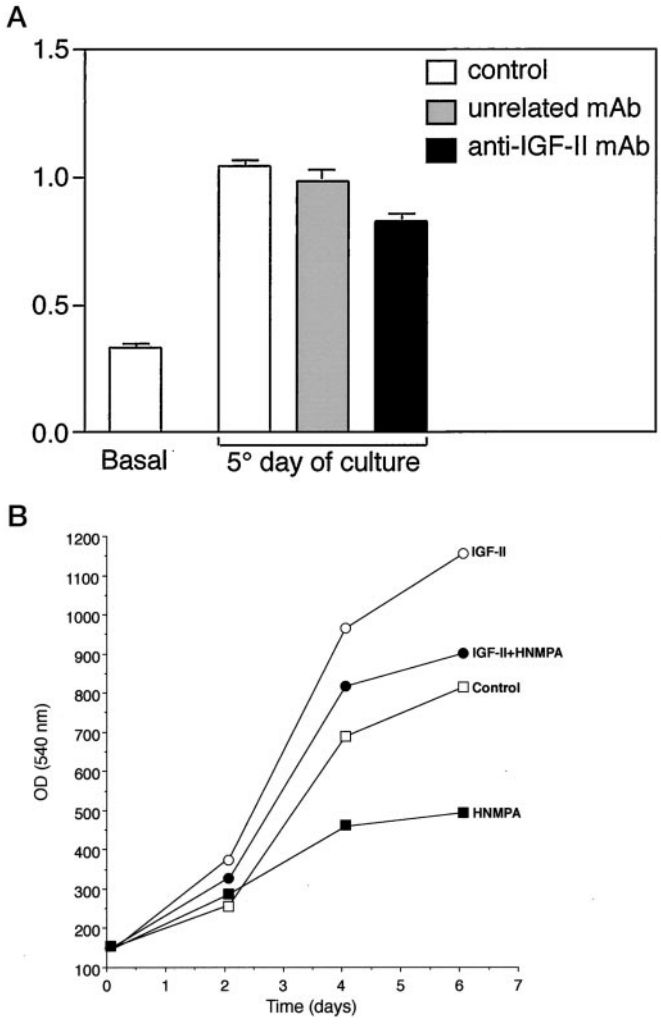

FIG. 6. Thyroid cancer cell growth after interruption of the IGF-II/IR-A autocrine loop. A, By an IGF-II blocking antibody. B-CPAP cells were seeded in monolayer cultures, and cell proliferation was measured after 5 d of culture, in the presence of either a blocking antibody to IGF-II or an unrelated monoclonal antibody (control cultures). Cell growth was significantly reduced in cultures treated with anti-IGF-II antibody compared with control cultures ($P = 0.0016$). Results are the mean ± SD of three separate experiments. B, By IR tyrosine kinase inhibitor HNMPA. HNMPA markedly inhibited B-CPAP cell growth in response to 10 nM IGF-II and reduced unstimulated cell growth most likely due to IR stimulation by autocrine IGF-II production.

the autocrine IGF-II/IR-A loop on spontaneous cell growth. First, B-CPAP were cultured in serum-free medium in either the presence or absence of an IGF-II-blocking antibody. After 5 d in culture cell proliferation was significantly decreased by the IGF-II-blocking antibody compared with normal mouse IgGs (−26%; $P = 0.0016$).

Next, we evaluated the effect of HNMPA, a specific IR tyrosine kinase inhibitor. HNMPA (1.0 nM) markedly inhibited the growth of serum-starved B-CPAP cells in response to 10 nM exogenous IGF-II (Fig. 6). Spontaneous cell growth was also significantly reduced by the presence of 1.0 nM HNMPA (Fig. 6), suggesting that IR tyrosine kinase inhibition blocks cell growth induced by autocrine IGF-II production. Very similar results were obtained with ARO cells (data not shown).

TABLE 5. Total IR content and proportion of IR-A in normal thyroid tissue and cancer thyroid tissue specimens

	IR (ELISA; ng/100 μg protein)	IR-A (RT-PCR; %)
Normal thyroid (n = 6)		
Mean ± SD	1.3 ± 0.5	45.2 ± 3.9
Range	0.7–2.1	40.0–50.5
Median	1.3	44.3
Papillary cancer (n = 14)		
Mean ± SD	5.8 ± 3.8	53.5 ± 5.7
Range	1.8–16.8	40.5–60.5
Median	5.7	53
Follicular cancer (n = 4; poorly differentiated)		
Mean ± SD	10.8 ± 8.6	56.6 ± 7.1
Range	5.2–23.7	49.5–65
Median	7.2	56
Anaplastic cancer (n = 4)		
Mean ± SD	12.6 ± 9.6	69.4 ± 4.3
Range	6.6–26.7	60.3–73.0
Median	9.6	70.5

IR content: normal *vs.* cancer (total), $P = 0.0007$ (by Mann-Whitney test); normal *vs.* papillary *vs.* follicular *vs.* anaplastic cancer, $P = 0.013$ (by one-way ANOVA).

IR and IGF-I-R expression and IR-A relative abundance in thyroid tissue specimens obtained at surgery. To investigate the potential *in vivo* relevance of the IGF-II/IR-A interaction in human thyroid carcinomas, we measured the IR content and the relative abundance of the two IR isoforms in surgical specimens of normal thyroid (n = 6) and cancer thyroid tissues (papillary, n = 14; follicular, n = 4; anaplastic, n = 4).

The total IR content was elevated in cancer specimens of all histotypes (range, 1.8–26.7 ng/100 μg cell membrane protein) compared with normal thyroid specimens (range, 0.7–2.1 ng/100 μg cell membrane protein; Table 5). Median IR values were increased approximately 4-fold in differentiated cancers and 8- to 10-fold in poorly differentiated and undifferentiated cancers. The IR-A transcript accounted for 40.0–50.5% (median, 44.3%) of total IR in normal thyroid tissues, whereas it ranged from 40.5–73% (median, 55.7%) in cancer specimens. This difference is highly significant ($P = 0.006$). Poorly differentiated and undifferentiated carcinomas expressed both higher total IR content and relative abundance of IR isoform A compared with well differentiated papillary carcinomas ($P = 0.005$; Table 5).

In four cases of papillary carcinomas, paired specimens of cancer and normal thyroid tissue from the same patients were available; the proportion of the IR-A transcript in cancer tissues clearly exceeded that in adjacent normal tissues in three cases, and it was similar in one case (Fig. 7).

To evaluate the relative contributions of IR and IGF-I-R in the activation of the IGF system in thyroid cancer, we also measured IGF-I-R content in the same thyroid specimens. IGF-I-R was 5.2 ± 1.9 ng/100 μg cell membrane protein in normal thyroid specimens and increased to 9.8 ± 4.3 in papillary cancer, but was not increased in poorly differentiated and undifferentiated carcinomas (5.2 ± 1.6 and 6.6 ± 4.5 ng/100 μg cell membrane protein, respectively).

Taken together these data indicate that IR-A, but not IGF-I-R, overexpression is the key factor of IGF system activation in both poorly differentiated and undifferentiated thyroid cancers. Even in differentiated cancers the increase in IR-A is more marked than that in IGF-I-R.

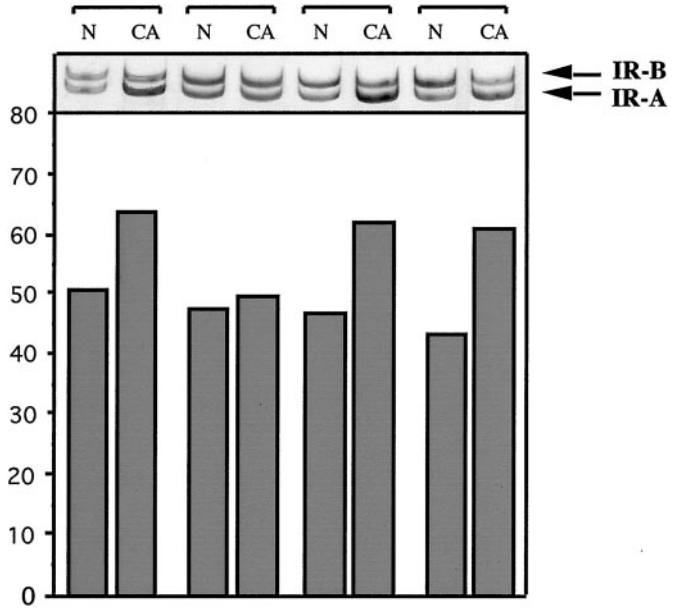

FIG. 7. IR-A transcript relative abundance in paired specimens of normal and cancer thyroid tissue. IR isoform mRNA expression in four specimens of papillary carcinomas (CA) and in the contralateral normal thyroid tissues (N). Products of PCR amplification were resolved by electrophoresis on 5% polyacrylamide gels and silver stained. IR-A relative abundance in paired normal and cancer thyroid tissues was quantified by scanning densitometry. Results are representative of three separate experiments.

Discussion

IGF-I and IGF-II are believed to play an important role in cancer progression and malignant cell protection from apoptosis (39–41), as they may be locally produced in tumors and exert their autocrine or paracrine action by binding to and activating the IGF-I-R (15).

We previously observed that IGF-I is overproduced in human thyroid cancer in a paracrine fashion and that the IGF-I-R homolog IR plays a role in mediating the IGF-I response. In fact, IR is overexpressed in most thyroid cancer cells (11) and thyroid cancer tissue specimens and amplifies the biological effects of IGF-I by forming hybrid IR/IGF-I-R receptors that bind IGF-I with high affinity (17). By this mechanism IR overexpression also causes a marked increase in IGF-I-binding sites in those cancers that do not overexpress IGF-I-Rs.

Here we demonstrate that IR overexpression may also directly increase the thyroid cancer cell response to IGF-II by activating a newly recognized autocrine loop involving IR-A, which behaves as a high affinity IGF-II-R. Differential splicing of IR mRNA is tightly regulated in a tissue-specific manner, generating various proportions of IR-A and IR-B isoforms (23). We recently demonstrated that isoform A, but not isoform B, is a physiological receptor for IGF-II in fetal tissues (22), where IR-A is predominantly expressed, whereas IR-B is predominantly expressed in adult tissues. These findings provide a mechanistic basis to studies suggesting that during fetal development the growth-promoting effect of IGF-II is partially mediated by signaling through the IR (22). We also observed that IR-A might be the predominant isoform expressed in major human carcinomas (22, 24). In breast cancer, however, IGF-II is mainly produced in a paracrine manner, and the relative abundance of IR-A appears not to be related to tumor stage, grading, or ER status (24). Further studies, however, are needed to assess the clinical relevance of IR-A in breast cancer.

In contrast, in the thyroid model, the relative abundance of IR-A progressively increases from normal thyrocytes (that predominantly express IR isoform B) to differentiated papillary thyroid cancer cells, to undifferentiated thyroid cancer cells that express a very high (>70%) IR-A proportion. Autocrine IGF-II production is also activated in thyroid cancer cells and follows the same expression pattern as IR-A, being especially elevated in poorly differentiated tumors. In contrast, primary cultures from normal thyroid produced IGF-II in only in 7 of 11 cases and only in small amounts. IR activation by IGF-II is directly and significantly related to the relative abundance of IR-A.

Therefore, in thyroid cancer this newly identified autocrine loop involving IGF-II and IR-A appears particularly relevant in poorly differentiated thyroid cancers. The biological relevance of the IGF-II/IR-A loop in thyroid cancer is confirmed by the observation that blockade of either IGF-II or IR, by multiple approaches, significantly reduces thyroid cancer cell growth induced by either exogenous or autocrine IGF-II.

In contrast to IRs, IGF-I-Rs are overexpressed only in well differentiated thyroid papillary tumors where paracrine IGF-I secretion is also increased (17), but not in poorly differentiated or undifferentiated tumors, where paracrine IGF-I secretion is rarely increased (17).

Taken together these studies indicate that IR-A overexpression is a major determinant for the overactivation of the IGF system in poorly differentiated thyroid cancer, both by activating the autocrine loop involving IGF-II and by contributing to the paracrine loop involving IGF-I, via the formation of IR/IGF-I-R hybrids (17). In differentiated thyroid cancer, both the paracrine IGF-I/IGF-I-R loop and, to a lesser extent, the autocrine IGF-II/IR-A loop are activated.

In addition to the specific growth factor (TSH), therefore, a variety of growth factors (IGF-I and IGF-II, hepatocyte growth factor, epidermal growth factor, and fibroblast growth factor) and their tyrosine kinase receptors (4–10) may play an important role in thyroid cancer growth and progression. These mechanisms should be taken into account in thyroid tumors that progress despite TSH suppression, as therapeutic strategies that involve the interruption of these autocrine/paracrine loops may positively influence cancer biology and patient outcome.

Acknowledgments

We thank Dr. I. D. Goldfine (San Francisco, CA) and Dr. K. Siddle (Cambridge, UK) for kindly providing us with anti-IR and anti-IGF-I-R antibodies.

Received March 28, 2001. Accepted September 24, 2001.

Address all correspondence and requests for reprints to: Prof. Riccardo Vigneri, Cattedra di Endocrinologia, Ospedale Garibaldi, 95123 Catania, Italy. E-mail: vigneri@mbox.unict.it.

This work was supported in part by the Associazione Italiana per la Ricerca sul Cancro (to A.B. and R.V.) and MURST (Cofin99, to A.B.).

* Recipient of a fellowship from the Giuseppe Alazio Foundation for cancer research.

† Recipient of a Federazione Italiana per la Ricerca sul Cancro fellowship.

References

1. **Mazzaferri EL** 1993 Thyroid carcinoma: papillary and follicular. In: Mazzaferri L, Samaan NA, eds. Endocrine tumors. Cambridge: Blackwell; 278–333
2. **Farid NR, Shi Y, Zou M** 1994 Molecular basis of thyroid cancer. Endocr Rev 15:202–232
3. **Fagin JA** 1994 Molecular pathogenesis of human thyroid neoplasm. Thyroid Today 17:1–7
4. **Kanamori A, Abe Y, Yajima Y, Manabe Y, Ito K** 1989 Epidermal growth factor receptors in plasma membranes of normal and desease human thyroid glands. J Clin Endocrinol Metab 68:899–903
5. **Haugen DRF, Akslen LA, Varhaug JE, Lillehaug JR** 1992 Expression of c-erb B-2 protein in papillary thyroid carcinomas. Br J Cancer 65:832–837
6. **Grieco M, Santoro M, Berlingieri MT, Melillo RM, Donghi R, Bongarzone I, Pierotti MA, Della Porta G, Fusco A, Vecchio G** 1990 PTC is a novel rearranged form of the ret proto-oncogene and is frequently detected in vivo in human thyroid papillary carcinomas. Cell 60:557–563
7. **Greco A, Pierotti MA, Bongarzone I, Pagliardini S, Lanzi C, Della Porta G** 1992 TRK-T1 is a novel oncogene formed by the fusion of TPR and TRK genes in human papillary thyroid carcinomas. Oncogene 7: 237–242
8. **Belfiore A, Gangemi P, Costantino A, Russo G, Santonocito GM, Ippolito O, Di Renzo MF, Comoglio P, Fiumara A, Vigneri R** 1997 Low/absent expression of the Met/HGFR identifies papillary thyroid carcinomas with high risk of distant metastases. J Clin Endocrinol Metab 82:2322–2328
9. **Yashiro T, Ohba Y, Murakami H, Obara T, Tsushima T, Fujimoto Y, Shizume K, Ito K** 1989 Expression of insulin-like growth factor receptors in primary human thyroid neoplasm. Acta Endocrinol (Copenh) 121:112–120
10. **Eggo MC, Hokins JM, Franklyn JA, Johnson GD, Sanders DS, Sheppard MC** 1995 Expression of fibroblast growth factor in thyroid cancer. J Clin Endocrinol Metab 80:1006–1011
11. **Frittitta L, Sciacca L, Catalfamo R, Ippolito A, Gangemi P, Pezzino V, Filetti S, Vigneri R** 1999 Functional insulin receptors are overexpressed in thyroid tumors. Cancer 85:492–498
12. **Duh QY, Grossman RF** 1995 Thyroid growth factors, signal transduction pathways, and oncogenes. Surg Clin North Am 75:421–437
13. **Van der Laan BF, Freeman JL, Asa SL** 1995 Expression of growth factors and growth factor receptors in normal and tumorous human thyroid tissues. Thyroid 5:67–73
14. **Le Roith D, Baserga R, Helman L, Roberts Jr CT** 1995 Insulin-like growth factors and cancer. Ann Intern Med 122:54–59
15. **Ullrich, A, Gray, A, Tam, AW, Yang-Feng T, Tsubokawa M, Collins C, Henzel W, Le Bon T, Kathuria S, Chen E** 1986 Insulin-like growth factor I receptor primary structure: comparison with insulin receptor suggests structural determinants that define functional specificity. EMBO J 5:2503–2512
16. **Steele-Perkins G, Turner J, Edman JC, Hari J, Pierce SB, Stover C, Rutter WJ, Roth RA** 1988 Expression and characterization of a functional human insulin-like growth factor I receptor. J Biol Chem 263:11486–11492
17. **Belfiore A, Pandini G, Vella V, Squatrito S, Vigneri R** 1999 Insulin/IGF-I receptors play a major role in IGF-I signaling in thyroid cancer. Biochimie 81:403–407
18. **Soos WA, Whittaker J, Lammers R, Ullrich A, Siddle K** 1990 Receptors for insulin and insulin-like growth factor-I can form hybrid dimers. Biochem J 270:383–390
19. **Jonas HA, Cox AJ, Harrison LC** 1989 Delineation of atypical insulin receptors from classical insulin and type I insulin-like growth factors receptors in human placenta. Biochem J 257:101–107
20. **Jonas HA, Cox AJ** 1990 Insulin-like growth factor binding to the atypical insulin receptors of a human lymphoid-derived cell line (IM-9). Biochem J 266:737–742
21. **Morrione A, Valentinis B, Xu S-q, Yumet G, Louvi A, Efstratiadis A, Baserga R** 1997 Insulin-like growth factor II stimulates cell proliferation through the insulin receptor. Proc Natl Acad Sci USA 94:3777–3782
22. **Frasca F, Pandini G, Scalia P, Sciacca L, Mineo R, Costantino A, Goldfine ID, Belfiore A, Vigneri R** 1999 Insulin receptor isoform A, a newly recognized high affinity insulin-like growth factor II receptor in fetal and cancer cells. Mol Cell Biol 19:3278–3288
23. **Moller DE, Yokota A, Caro JF, Flier JS** 1989 Tissue-specific expression of two alternatively spliced insulin receptor mRNAs in man. Mol Endocrinol 3:1263–1269
24. **Sciacca L, Costantino A, Pandini G, Mineo R, Frasca F, Scalia P, Sbraccia P, Goldfine ID, Vigneri R, Belfiore A** 1999 Insulin receptor activation by IGF-II in breast cancers: evidence for a new autocrine/paracrine mechanism. Oncogene 18:2471–2479
25. **Roth RA, Cassel DJ, Wong KY, Maddux BA, Goldfine ID** 1982 Monoclonal antibodies to the human insulin receptor block insulin binding and inhibit insulin action. Proc Natl Acad Sci USA 79:7312–7316
26. **Forsayeth JR, Montemurro A, Maddux BA, DePirro R, Goldfine ID** 1987 Effect of monoclonal antibodies on human insulin receptor autophosphorylation, negative cooperativity, and down-regulation. J Biol Chem 262:4134–4140
27. **Ganderton RH, Stanley KK, Field CE, Coghlan MP, Soos MA, Siddle K** 1992 A monoclonal anti-peptide antibody reacting with the insulin receptor β-subunit. Biochem J 288:195–205
28. **Soos MA, Siddle K, Baron MD, Heward JM, Luzio JP, Bellatin J, Lennox ES** 1986 Monoclonal antibodies reacting with multiple epitopes on the human insulin receptor Biochem J 235:199–208
29. **Kull FC Jr, Jacobs S, Su YF, Svoboda ME, Van Wyk JJ, Cuatrecasas P** 1983 Molecolar antibodies to receptors for insulin and somatomedin C. J Biol Chem 258:6561–6566
30. **Milazzo G, La Rosa GL, Catalfamo R, Vigneri R, Belfiore A** 1992 Effect of TSH in human thyroid cells: evidence for both mitogenic and antimitogenic effect. J Cell Biochem 49:231–238
31. **Estour B, Van Herle AJ, Juillard GJF, Totanes TL, Sparkes RS, Giuliano AE, Klandorf H** 1989 Characterization of a human follicular thyroid carcinoma cell line (UCLA RO 82 W-1). Virchows Arch B Cell Pathol 57:167–174
32. **Tanaka J, Ogura T, Sato H, Hatano M** 1987 Establishment and biological characterization of an in vitro human cytomegalovirus latency model. Virology 161:62–72
33. **Fabien N, Fusco A, Santoro M, Barbier Y, Dubois PM, Paulin C** 1994 Description of a human papillary thyroid carcinoma cell line. Cancer 73:2206–2212
34. **Ebina Y, Ellis L, Jarnaglin K, Edery M, Graf L, Clauser E, Ou JH, Masiarz F, Kan YW, Goldfine ID** 1985 The human insulin receptor cDNA: the structural basis for hormone-activated transmembrane signalling. Cell 40:747–758
35. **Belfiore A, Costantino A, Frasca F, Pandini G, Mineo R, Vigneri P, Maddux B, Goldfine ID, Vigneri R** 1996 Overexpression of membrane glycoprotein PC-1 in insulin-resistant MDA-MB231 human breast cancer cells. Mol Endocrinol 10: 1318–1326
36. **Giorgino F, Belfiore A, Milazzo G, Costantino A, Maddux B, Whittaker J, Goldfine ID, Vigneri R** 1991 Overexpression of insulin receptors in fibroblast and ovary cells induces a ligand-mediated transformed phenotype. Mol Endocrinol 5:452–459
37. **Heo DS, Park J-G, Hata K, Day R, Herberman RB, Whiteside TL** 1990 Evaluation of tetrazolium-based semiautomatic colorimetric assay for measurement of human antitumor cytotoxicity. Cancer Res 50:3681–3690
38. **Baltensperger K, Lewis RE, Woon CW, Vissavajjhala P, Ross AH, Czech MP** 1992 Catalysis of serine and tyrosine autophosphorilation by the human insulin receptor. Proc Natl Acad Sci USA 89:7885–7889
39. **Humbel RE** 1990 Insulin-like growth factors I and II. Eur J Biochem 190: 445–462
40. **Baserga R** 1995 The insulin-like growth factor I receptor: a key to tumor growth? Cancer Res 55:249–252
41. **Macaulay VM** 1992 Insulin-like growth factors and cancer. Br J Cancer 65: 311–320